Cell, Vol. 119, 245–256, October 15, 2004, Copyright ©2004 by Cell Press

Control of Dendritic Branching and Tiling by the Tricornered-Kinase/Furry Signaling Pathway in *Drosophila* Sensory Neurons

Kazuo Emoto,[1] Ying He,[2] Bing Ye,[1] Wesley B. Grueber,[1] Paul N. Adler,[2] Lily Yeh Jan,[1] and Yuh-Nung Jan[1,*]

[1]Howard Hughes Medical Institute
Department of Physiology and Biochemistry
University of California San Francisco
1550 4th Street
San Francisco, California 94143

[2]Biology Department and Cancer Center
University of Virginia
Charlottesville, Virginia 22903

Summary

To cover the receptive field completely but without redundancy, neurons of certain functional groups exhibit tiling of their dendrites via dendritic repulsion. Here we show that two evolutionarily conserved proteins, the Tricornered (Trc) kinase and Furry (Fry), are essential for tiling and branching control of *Drosophila* sensory neuron dendrites. Dendrites of *fry* and *trc* mutants display excessive terminal branching and fail to avoid homologous dendritic branches, resulting in significant overlap of the dendritic fields. Trc control of dendritic branching involves regulation of RacGTPase, a pathway distinct from the action of Trc in tiling. Time-lapse analysis further reveals a specific loss of the ability of growing dendrites to turn away from nearby dendritic branches in *fry* mutants, suggestive of a defect in like-repels-like avoidance. Thus, the Trc/Fry signaling pathway plays a key role in patterning dendritic fields by promoting avoidance between homologous dendrites as well as by limiting dendritic branching.

Introduction

Precise patterning of the dendritic fields is essential for the correct wiring of neuronal circuitry. Once the territory is covered by dendrites, the growth and branching of dendrites would stop normally, so as to prevent any overlap of the receptive fields of neighboring neurons and the consequent compromise of neuronal circuit properties. Indeed, diseases characterized by the formation of enlarged dendritic fields result in severe mental retardation (Purpura, 1975; Kaufmann and Moser, 2000). Notwithstanding recent progress in our knowledge of molecular mechanisms that promote dendritic elaboration (Cline, 2001; Scott and Luo, 2001; Whitford et al., 2002; Jan and Jan, 2003), the cellular and molecular mechanisms governing the dendritic field specification are still poorly understood.

Dendritic tiling refers to the complete but nonredundant coverage of a receptive field by dendrites of functionally homologous neurons, like tiles covering a floor (Jan and Jan, 2003). Tiling has been well characterized in the mammalian retina (Wässle et al., 1981; Perry and Linden, 1982; DeVries and Baylor, 1997; MacNeil and Masland, 1998; Lohmann and Wong, 2001). Retinal ganglion cells (RGCs) in the rabbit retina, for example, can be grouped into at least 11 distinct physiological classes (DeVries and Baylor, 1997). Dendrites of some RGCs of the same subtype typically cover the whole retina with minimal overlap, whereas dendrites of different subtypes overlap extensively. Similarly, amacrine cells in the rabbit retina are classified into at least 22 subclasses based on the branching pattern of their dendrites, and several subtypes appear to tile the retina (MacNeil and Masland, 1998). Tiling thus ensures efficient and unambiguous representation of the entire visual field and is likely to be of general importance. Indeed, dendritic tiling among sensory neurons of moths and flies suggest that tiling is an evolutionarily conserved mechanism for dendritic field organization (Grueber et al., 2001, 2002).

Drosophila dendrite arborization (da) sensory neurons provide a suitable system to study cellular and molecular mechanisms underlying dendritic development (Bodmer and Jan, 1987; Gao et al., 1999). The 15 da neurons in each abdominal hemisegment are classified into four subtypes based on their unique dendritic arborization profiles (Grueber et al., 2002). In addition, class III and class IV da neurons exhibit tiling in a subtype-specific manner (Grueber et al., 2002; Sugimura et al., 2003). Several lines of evidence suggest that the dendritic tiling of class IV neurons arises from class-specific competition between dendrites of neighboring neurons. First, dendrites of class IV neurons often appear to stop growing, make a turn, or retract as they come within a short distance of each other, whereas there is extensive overlap between dendrites of neurons belonging to different classes (Grueber et al., 2002, 2003a; Sugimura et al., 2003). Second, laser ablation of certain class IV neurons during late embryonic stages causes dendrites of the surrounding class IV neurons to grow into the territories of the ablated neurons (Grueber et al., 2003a; Sugimura et al., 2003). Conversely, duplication of a class IV neuron results in a reduction rather than any overlap of their respective fields (Grueber et al., 2003a). Third, despite the dendritic overgrowth and/or overbranching in mutants (Gao et al., 1999), such as *flamingo* (Gao et al., 2000) and *sequoia* (Brenman et al., 2001), there is still tiling between the extra branches within the same neuron as well as between different neurons (Grueber et al., 2002). These observations suggest that a like-repels-like mechanism is responsible for the dendritic tiling of class IV neurons; however, the underlying molecular mechanisms remain unknown.

tricornered (trc) and *furry (fry)* are evolutionally conserved genes implicated in regulating cell morphology (Adler, 2002). The *trc* and *fry* genes encode a serine/threonine kinase of the ACG family (Tamaskovic et al., 2003) and a large (~380 kDa) protein with no known functional domain (Cong et al., 2001), respectively. In budding yeast, the Trc homolog Cbk1p promotes nuclear translocation of the Ace2p transcription factor, which controls the daughter cell-specific expression of

*Correspondence: ynjan@itsa.ucsf.edu

cell separation genes (Colman-Lerner et al., 2001; Weiss et al., 2002). Cbk1p also controls polarized cell growth through an Ace2p-independent mechanism (Colman-Lerner et al., 2001; Weiss et al., 2002). The Fry homolog Tao3p (also named Pag1p) is required for both Cbk1p functions (Du and Novick, 2002; Nelson et al., 2003). Mutation of a fungal homolog of *trc*, *cot1*, causes a drastic increase of the hyphal branching in *Neurospora* (Yarden et al., 1992). Interestingly, mutations of the *trc* homolog *sax-1* in *C. elegans* cause sensory neurons to have ectopic neurites (Zallen et al., 2000). In *Drosophila*, mutations of either *trc* or *fry* result in branched bristles and multiple wing hair phenotypes (Geng et al., 2000; Cong et al., 2001). However, the roles of Trc and Fry in neurons are obscure.

In this study we show that Trc and Fry function cell autonomously in *Drosophila* da neurons to regulate dendritic tiling and branching. Trc-kinase activity is required for the dendritic branching and tiling in vivo and is positively regulated by Fry. The control of dendritic branching but not tiling involves negative regulation of the RacGTPase signaling pathway by Trc. These findings suggest that Trc/Fry utilizes two distinct signaling pathways to shape the dendritic fields: one pathway to limit dendritic branching and a separate pathway to promote like-repels-like response of dendritic processes.

Results

trc and *fry* Mutants Display Dendritic Branching Phenotypes

In a screen for enhancer trap lines showing expression in dendrite arborization (da) neurons, we found one insertion line termed KY319 with high expression in da neurons throughout the larval stages. Genomic DNA flaking the P element was isolated by plasmid rescue and the P element was found to be inserted in the first intron of the *fry* gene. Because the *fry* mutants were known to have branched bristles and multiple wing hair phenotypes (Cong et al., 2001; Adler, 2002), we decided to explore *fry*'s potential role in the control of the dendritic morphogenesis of da neurons.

To visualize dendrites in *fry* mutants, we introduced the *pickpocket*-EGFP reporter, which is specifically expressed in class IV sensory neurons (Grueber et al., 2003a), into each *fry* mutant allele. We found that *fry* mutant neurons exhibited excessive dendritic branches. In the wild-type third instar larvae, class IV ddaC neurons in the dorsal cluster elaborate highly complex but stereotyped dendritic trees and extend a single axon ventrally (Figures 1A and 4A); the ddaC dendrites normally display a consistent number of terminal branches (Grueber et al., 2003b; Ye et al., 2004). In the *fry* null mutant (*fry*^{1}), both the terminal branch number and the total branch length were increased by a factor of two, whereas the major branch architecture appeared normal (Figures 1B, 1E, and 1F). This branching phenotype of *fry* mutants was already apparent in early first instar larvae, and the terminal branch number of the mutants was almost twice that of wild-type in the first, second, and third instar larval stages (data not shown).

The *fry* gene functions together with the *trc* gene to control wing hair and bristle morphology (Geng et al., 2000; Cong et al., 2001). In addition, *fry* homologs show strong genetic interactions with *trc* homologs in a variety of species including *S. cerevisiae* (Du and Novick, 2002; Nelson et al., 2003), *S. pombe* (Hirata et al., 2002), and *C. elegans* (Zallen et al., 2000). To test whether *trc* is also involved in controlling dendritic branching in neurons, we examined ddaC dendrites of a *trc* null mutant (*trc*^{1}) and found that the *trc* dendrites displayed overbranching phenotypes similar to those of *fry* mutants (Figures 1D and 1E). These observations suggest that both *trc* and *fry* function to regulate dendritic branching of class IV da neurons.

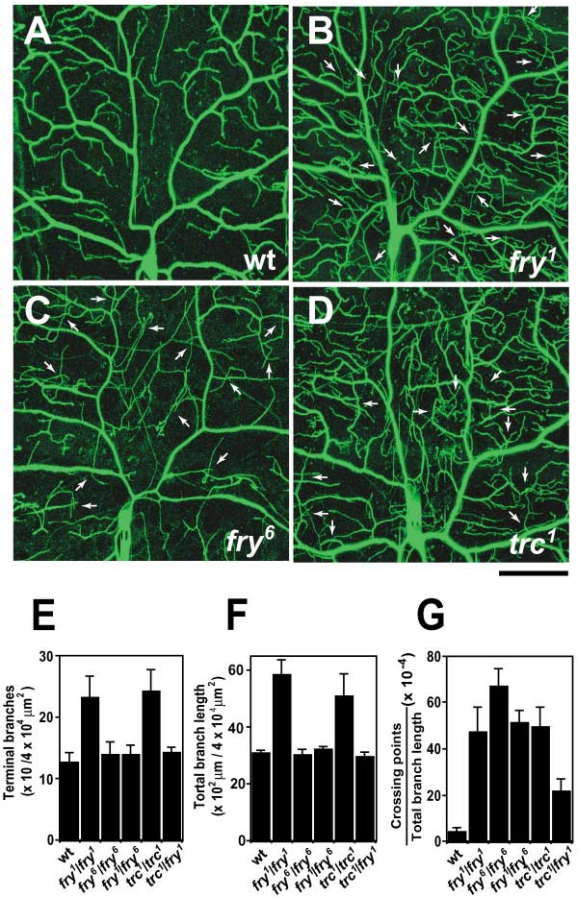

Figure 1. *trc* and *fry* Mutants Exhibit Supernumerary Terminal Branching and Defective Dendritic Tiling

(A–D) Live images of ddaC dendrites visualized by *pickpocket*-EGFP reporter in wild-type (A), *fry*^{1} homozygote (B), *fry*^{6} homozygote (C), and *trc*^{1} homozygote (D). Anterior is left and dorsal is up. Arrows indicate crossing points of terminal dendrites. Scale bars represent 50 μm.

(E–G) Quantification of the terminal branch number (E), the total branch length (F), and the crossing points normalized to the total dendritic branch length (G) of wild-type and mutant ddaC dendrites. (wt, n = 24; *fry*^{1}, *fry*^{6}, n = 25; *trc*^{1}, n = 15).

Dendritic Tiling Defect in a Class IV Neuron of *trc* and *fry* Mutants

Recent studies show that class IV da neurons exhibit dendritic tiling, presumably by exclusion between the terminal branches (Grueber et al., 2003a; Sugimura et

al., 2003). Indeed, the terminal branches of the same ddaC neuron typically stopped growing or turned away before crossing each other, resulting in minimum overlap (Figure 1A). In contrast, the dendritic branches of *fry*^{1} and *trc*^{1} ddaC neurons often overlapped each other (Figures 1B and 1D, arrows). Approximately 13% (*fry*^{1}, 12.5% $\pm$ 0.8%, n = 25; *trc*^{1}, 13.4% $\pm$ 1.2%, n = 15) of dendritic terminal branches crossed one another in *fry*^{1} and *trc*^{1} ddaC dendrites, compared to $\sim$1% (1.0 $\pm$ 0.3%, n = 24) of crossing in wild-type dendrites. The crossing branches of *fry* and *trc* mutants displayed rigid and straight trajectories (Figures 1B and 1D, arrows), implying an impairment in like-repels-like navigation. Because these terminal branches were sandwiched between the epidermis and muscles, which were typically less than 1 μm apart in both mutant and wild-type larvae, the excessive overlap of mutant dendrites is unlikely to result from abnormal stratification of terminal branches. These findings suggest that *trc* and *fry* are involved in regulation of the dendritic tiling in class IV neurons.

Tiling Phenotype Can Be Observed without Overbranching Defect

Since *trc* and *fry* null mutants displayed dendritic branching and tiling phenotypes, we wondered whether the tiling phenotype in mutants might simply arise from the excessive branching of terminal dendrites. To address this possibility, we normalized the number of dendritic crossings by the branch number (Figure 1E) and total dendrite length (Figure 1F) and found that the normalized dendritic crossings remained significantly increased in *fry* and *trc* mutants (Figure 1G).

We also examined the class IV dendrites of hypomorphic alleles and transheterozygotes of *trc* and *fry* and found that robust tiling phenotypes were still observed in mild mutants with *fry* and/or *trc* function reduced to a level that caused no overbranching (Figures 1E–1G). For instance, the *fry*^{6} hypomorphic allele shows a reduced *fry* expression due to a P element insertion (Cong et al., 2001). The *pickpocket*-EGFP reporter revealed that the *fry*^{6} mutant exhibited a clear tiling defect whereas the terminal branch number appeared unaffected (Figures 1C, arrows, 1E, and 1F). Indeed, normalized to the total branch length, the number of dendritic crossings in the *fry*^{6} mutant dendrites was slightly higher ($\sim$20%) than that in null mutants (Figure 1G). Similarly, tiling defect was apparent in larvae transheterozygous for *fry*^{1} and *fry*^{6} or *fry*^{1} and *trc*^{1} despite the normal dendritic length and branch points (Figures 1E–1G). Taken together, these observations suggest that the tiling phenotype in *trc* and *fry* mutants is not secondary to the overbranching phenotype and that *trc* and *fry* function together to ensure dendritic tiling of class IV neurons.

Trc and Fry Function Cell Autonomously in Controlling Dendritic Branching and Tiling

To determine whether *trc* and *fry* act cell autonomously in neurons, we used the MARCM (*m*osaic *a*nalysis with a *r*epressive *c*ell *m*arker) system (Lee and Luo, 1999) to generate mCD8-GFP-labeled *trc*, *fry*, or *trc fry* double mutant clones in heterozygous background. Compared to the wild-type ddaC dendrites, *trc* and *fry* mutant ddaC dendrites displayed a 50% increase in the number of branches (Figures 2A–2D; wt, 376 $\pm$ 31.3, n = 5; *trc*, 572 $\pm$ 86.9, n = 8; *fry*, 523 $\pm$ 41.3, n = 7). Moreover, mutant clones exhibited a tiling defect (Figures 2A–2C and 2E). A similar phenotype was observed in two ventral class IV MARCM clones (data not shown). The phenotypes of mutant clones were less severe than those seen in null mutant animals, presumably due to perdurance of wild-type proteins (Lee and Luo, 1999; Lee et al., 2000). The dendritic phenotypes of *trc fry* double mutant clones were indistinguishable from those of *trc* or *fry* single mutant clones (Figures 2D and 2E, branching points, 544 $\pm$ 53.1; n = 4). These results indicate that Trc and Fry act cell autonomously to regulate dendritic branching and tiling of class IV neurons.

Similarly, mutant clones of da neurons of class I (Figures 3A–3C and 3J), class II (Figures 3D–3F and 3K), and class III (Figures 3G–3I and 3L) also showed a 2- to 3-fold increase in the number of terminal dendritic branches. In contrast to the drastic phenotypes in terminal branches, the major dendritic branch architecture including primary, secondary, and tertiary branches, as well as the cell body shape were not obviously affected. Furthermore, the *trc*, *fry*, and double mutant clones showed no detectable defects in bipolar dendrite neurons, external sensory neurons, or chordotonal neurons (data not shown). Thus, among sensory neurons, *trc* and *fry* specifically control the terminal branching of da neuron dendrites.

Trc and Fry Control Dendritic Tiling between Different Class IV Neurons

Given that *trc* and *fry* mutations compromised tiling of terminal branches from the same neuron (iso-neuronal tiling), we wondered whether *trc* and *fry* also control tiling of dendrites from different neurons (hetero-neuronal tiling). The dendrites of the three class IV neurons in each abdominal hemisegment, ddaC, v'ada, and vdaB (Figure 4A), normally cover the whole epidermis with minimal overlap (Grueber et al., 2002, 2003a; Sugimura et al., 2003). For example, the adjacent v'ada and vdaB neurons appeared to respect the respective dendritic territories and rarely sent their dendrites into the dendritic fields of their neighbors (Figures 4B and 4C). In *fry*^{1} and *trc*^{1} null mutants, however, the v'ada and vdaB dendrites often invaded neighboring fields, resulting in a partial overlap of the dendritic fields (Figures 4D, 4E, 4H, and 4I). Major branches as well as terminal branches overlapped extensively in both *fry* and *trc* mutants. The *fry*^{6} hypomorphic mutant also displayed clear hetero-neuronal tiling defects (Figures 4F and 4G). Similar but milder dendritic tiling defects were observed in transheterozygotes for *fry*^{1} and *fry*^{6} and in transheterozygotes for *fry*^{1} and *trc*^{1} (Figure 4J). As observed in ddaC neurons, v'ada and vdaB dendrites also displayed iso-neuronal tiling defects with 12%–14% crossing in *fry* and *trc* mutants (*fry*^{1}, 12.1% $\pm$ 0.4%, n = 25; *trc*^{1}, 14.1% $\pm$ 0.8%, n = 15), compared to only 1% crossing in the wild-type control (1.1% $\pm$ 0.2%, n = 25) (Figures 4B–4I, arrows). There was a good correlation between the strength of the iso-neuronal and hetero-neuronal tiling phenotypes (Figure 4J). These observations suggest that *trc* and *fry* regulate both iso-neuronal and hetero-neuronal tiling, presumably through the same mechanisms.

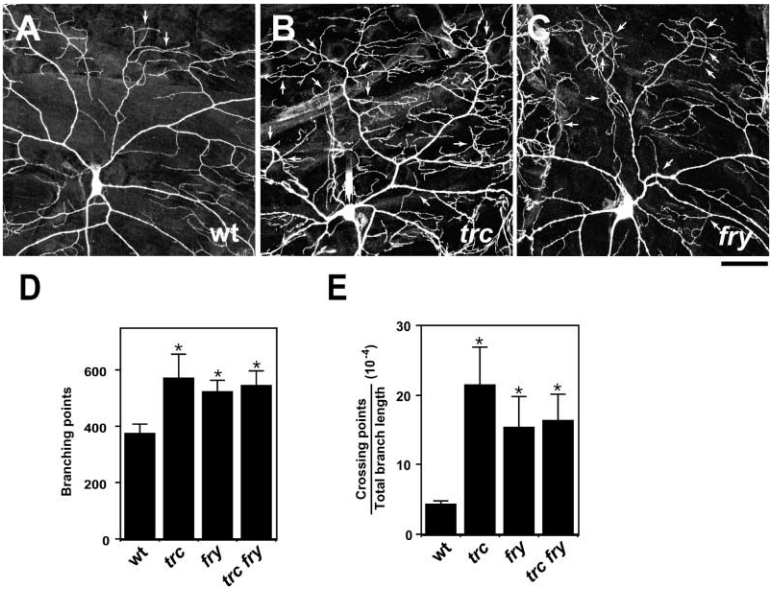

Figure 2. *trc* and *fry* Function Cell Autonomously in Regulation of Branching and Tiling in Class IV Neurons

MARCM clones of wild-type (A), trc^1 (B), and fry^1 (C) are shown. Arrows indicate crossing points of dendrites. Double mutant was generated by recombination of fry^1 with trc^7, a *trc* null allele generated by a P element insertion. (D) Quantification of the branch points of MARCM clones (* different from wild-type, $p < 0.05$). (E) Quantification of crossing points normalized to the total branch length of MARCM clones (* different from wild-type, $p < 0.05$). Scale bars represent 50 μm.

Dendrites of *fry* Mutants Are Defective in Like-Repels-Like Response

How might *trc* and *fry* prevent overlap of like dendrites? A priori, it is conceivable that multiple dendritic branches initially coinnervate the same territory and have extensive crossings; tiling could result from retraction of some of these branches. Alternatively, in the like-repels-like scenario, dendrites interact with one another to avoid overlap and crossing throughout development.

To distinguish between these possibilities, we first looked for dendritic crossings during development. Within a few hours around the time of hatching (AEL 20–23 hr), the territories of v'ada and vdaB neurons become defined. In wild-type control, we found no significant overlap between dendrites of v'ada and vdaB neurons throughout development: in newly hatched larvae, first instar larvae 3 or 6 hr after hatching, second or third instar larvae (Figure 4K). In contrast, dendritic crossings were already evident in newly hatched *fry* mutant larvae, and the number of crossings increased continuously during larval development (Figure 4K). Thus, consistent with previous studies (Grueber et al., 2003a; Sugimura et al., 2003), dendrites normally avoid one another as they meet initially, without going through a noticeable period of coinnervation followed by pruning; *fry* mutations affect the mechanism underlying this avoidance.

To further define the cellular functions of *fry* and *trc* in dendritic tiling, we imaged the dendrites of live wild-type and *fry* mutants for 16 hr starting at the early second instar larval stage, when class IV neurons had stabilized their major arbors. Many of the terminal branches remained dynamic, however, from the beginning (Figure 5A) to the end (Figure 5B) of the 16 hr period. Nearly 75% (wt, 74.2%; fry^1, 77.7%; fry^6, 76.0%) of the dynamic branches displayed a net extension (marked in red in Figures 5C and 5F), whereas 25% showed a net retraction (marked in green in Figures 5C and 5F) in both wild-type (Figure 5C) and *fry* mutants (Figure 5F). In wild-type larvae, 73% ($n = 178$) of those branches that extended their tips close (< 5 μm) to other branches turned away, hence avoided crossing, and only 1% extended beyond other branches (Figures 5A–5C, arrowheads, Table 1). The percentage of branches making a turn was significantly reduced by a factor of three in both null and hypomorphic *fry* mutants (Table 1). Instead of turning, about 45% of the mutant dendritic branches ran across other branches at many locations (Figures 5D–5F arrows, Table 1). These findings are consistent with the like-repels-like scenario. It appears that in *fry* mutants, dendrites can grow and retract normally, but their inability to turn in order to avoid like dendrites results in tiling defects.

Trc and Fry Are Expressed in Dendrite Arborization Neurons

To examine the expression pattern of Trc and Fry, we performed immunostaining analyses on dissected larvae using polyclonal antibodies raised against Trc or Fry. We found that both Trc and Fry are widely expressed including all da neurons in third instar wild-type larvae (Figures 6A–6C). In da neurons, Trc and Fry are localized predominantly in the soma but are also detected in axons and dendritic branches. When Trc tagged with FLAG-epitope (FLAG-Trc) was expressed in ddaC neurons by a class IV neuron-specific Gal4 driver (Grueber et al., 2003b; Ye et al., 2004), FLAG-Trc was distributed in soma, axon, as well as dendritic branches, similar to the endogenous Trc localization (Figures 6D and 6E). The staining was specific for Trc or Fry because the signal was absent in null mutants (data not shown).

Trc-Kinase Activity Is Essential for Dendritic Branching and Tiling Control

To investigate the function of the Trc kinase in neurons, we expressed wild-type and mutant Trc in neurons of *trc* mutants and tested whether the *trc* mutant phenotype could be ameliorated. The kinase domains of Trc and its orthologs share 70%–80% amino acid identity (Tamaskovic et al., 2003). In addition, Trc has conserved

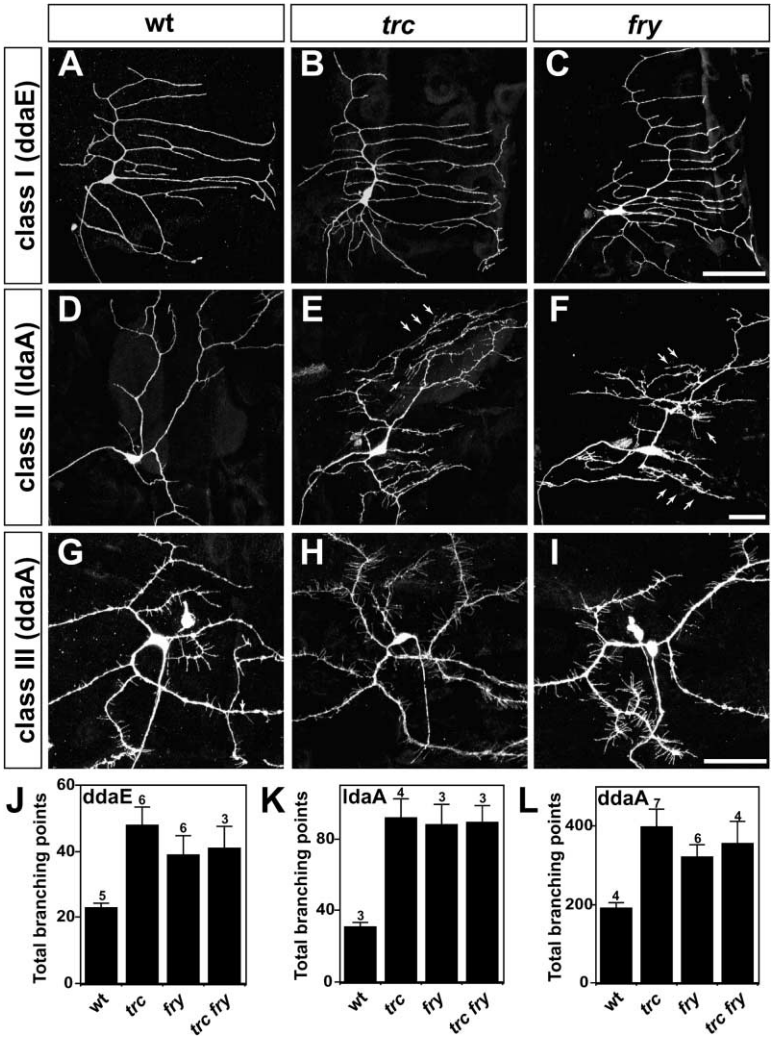

Figure 3. *trc* and *fry* Function Cell Autonomously in Regulation of Terminal Dendritic Branching in Class I, II, and III Da Neurons

(A–I) Mosaic clones of class I (ddaE) neurons (A–C), class II (ldaA) neurons (D–F), and class III (ddaA) neurons (G–I). Arrows point to ectopic dendritic branches. Clones of wild-type (A, D, and G), trc^1 (B, E, and H), and fry^1 (C, F, and I) were shown. Double mutant was generated by recombination of fry^1 with trc^7, a *trc* null allele generated by a P element insertion.

(J–L) Quantification of total branch number in class I (J), class II (K), and class III (L) MARCM clones. Numbers are the numbers of cells measured. Scale bars represent 50 μm.

phosphorylation sites at Ser292 and Thr449; phosphorylation at these residues is essential for maximal activation for the human Trc kinase in vitro (Millward et al., 1999; Tamaskovic et al., 2003) (Figure 7B). To test whether Trc kinase activity is required for proper dendritic branching and tiling in vivo, we generated a kinase-dead mutant (K122A) and a mutant in which both Ser292 and Thr449 were replaced with alanine (S292AT449A) to prevent phosphorylation. Specific expression of wild-type Trc with a class IV neuron-specific Gal4 driver largely rescued both dendritic branching and tiling defects of the trc^1 mutant (Figures 7D and 7I); however, neither the K122A nor the S292AT449A mutant could rescue these phenotypes (Figures 7E and 7I). These results suggest that Trc kinase activity in class IV neurons is important for their proper dendritic branching and tiling in vivo; this Trc activity is sufficient even in animals lacking Trc in other cell types.

Interestingly, overexpression of wild-type Trc in class IV neurons of wild-type larvae caused a slight reduction of branch number (Figure 7F). Moreover, expression of the K122A in wild-type class IV neurons resulted in a highly penetrant increase in terminal branches of ddaC dendrites as well as tiling defects similar to the phenotypes of *trc* and *fry* mutants (Figures 7G and 7J), indicating that the K112A acts as a dominant-negative mutant. Specific expression of the S292AT449A Trc mutant in wild-type class IV neurons also led to an increase of terminal dendrites, albeit milder than that induced by the K122A mutant, whereas the dendritic tiling defects seen in S292AT449A-expressing dendrites were as obvious as those induced by the K122A mutant (Figures 7H and 7J). These results strongly suggest that both Trc phosphorylation and Trc kinase activity in neurons play an essential role in dendritic branching and tiling.

Fry Positively Regulates Trc Kinase Activity

Given the genetic interaction between *trc* and *fry* and their evolutionarily conserved function in controlling branching of cellular processes, we investigated their functional relationship by assessing the Trc kinase activity in *trc* and *fry* mutants. Trc immunoprecipitates from wild-type, *trc*, or *fry* embryos were assayed for kinase activity by using histone H1 as an artificial substrate. Although similar amounts of Trc protein were precipitated from wild-type and *fry* homogenates, kinase activity of precipitates from *fry* mutants was significantly reduced, to the level similar to that of *trc* mutants (Figure

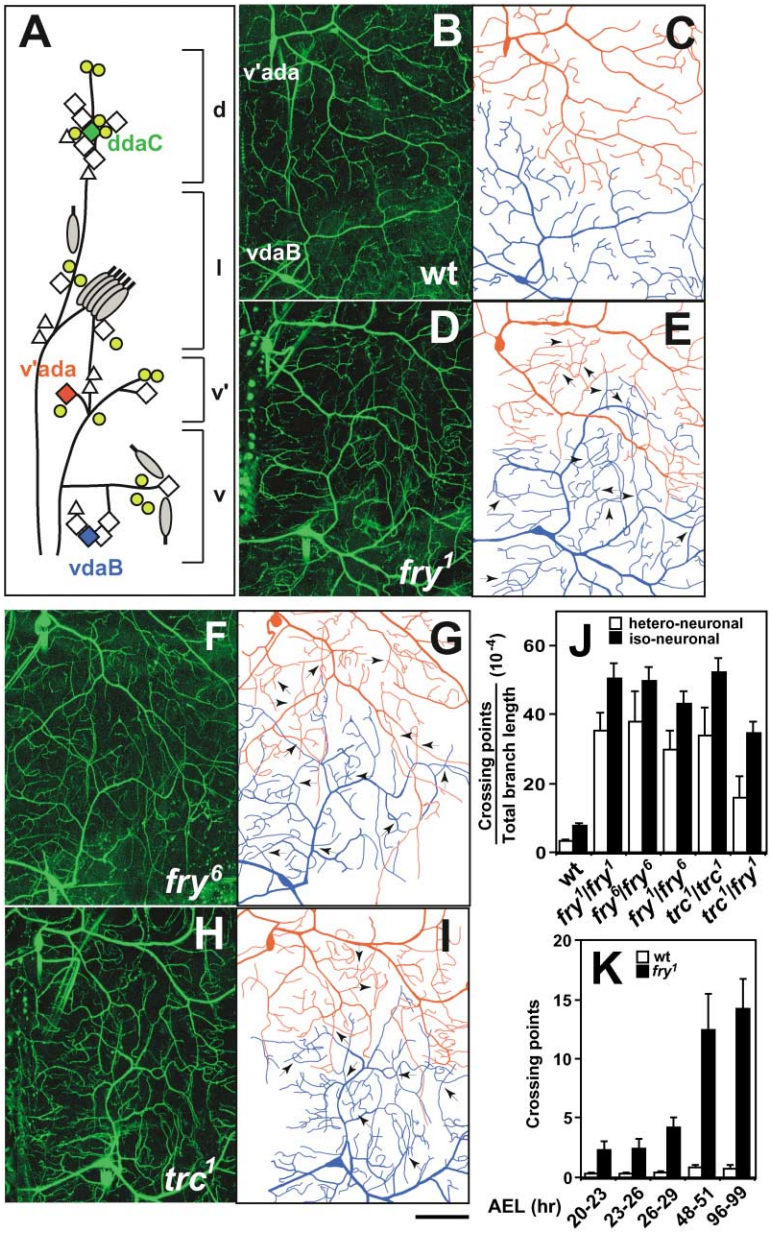

Figure 4. Hetero-Neuronal Dendritic Tiling Defect in *fry* and *trc* Mutants

(A) Schematic depiction of peripheral nervous system neurons in a single larval abdominal segment. Class IV neurons ddaC, v'ada, and vdaB are depicted in green, red, and blue diamonds, respectively. Other da neurons, diamonds; other multidendritic neurons, triangles; external sensory neurons, circles; chordotonal organs, gray. (B–I) Live images and their traces of v'ada, and vdaB dendrites. In wild-type larvae (B), dendrites of adjacent class IV neurons, v'ada and vdaB, do not overlap; however, class IV dendrites overlap extensively in fry^1 (D), fry^6 (F), and trc^1 (H) mutants, as evident from tracing of dendrites derived from v'ada (red) and vdaB (blue) in wild-type (C), fry^1 (E), fry^6 (G), and trc^1 (I) larvae. Arrows indicate crossing points of dendritic branches within the same neurons. The scale bar represents 50 μm.

(J) Quantification of the crossing points in v'ada and vdaB dendrites of the wild-type and the mutant third instar larvae (wt, fry^1, fry^6, n = 25; trc^1, n = 15). Crossing points are normalized to total dendritic length. White and black bars represent the dendritic crossing points between v'ada and vdaB neurons (hetero-neuronal) and within the same neurons (iso-neuronal), respectively.

(K) Quantification of the total crossing points between v'ada and vdaB dendrites of various larval stages (n = 25). The number represents the dendritic crossing points between v'ada and vdaB dendrites in wild-type (white bar) and fry^1 mutants (black bar).

7A). Since the Trc protein was undetectable in immunoprecipitates from *trc* embryos (Figure 7A), histone phosphorylation by precipitates from *trc* mutants is likely due to other kinases coprecipitated with the beads. These results indicate that the Trc kinase is inactive in *fry* mutants. Most likely, Trc kinase activity requires Fry and is a key component of a signaling pathway primed for refraining growth toward like structures and limiting branching.

Dendritic Branching but Not Tiling Depends on RacGTPase Regulation by Trc

The RhoGTPase family, including Rho, Rac, and Cdc42, plays a crucial role in neuronal morphogenesis (Redmond and Ghosh, 2001; Luo, 2002; Jan and Jan, 2003; Van Aelst and Cline, 2004). In particular, proper activation of Rac in developing neurons is essential for establishing and maintaining their unique dendritic branching pattern (Luo et al., 1994; Threadgill et al., 1997; Li et al., 2000; Nakayama et al., 2000; Lee et al., 2003). To test whether Trc signaling involves Rac regulation, we first asked whether overexpression of wild-type and mutant Rac1 affects dendritic morphology and then examined the effects of coexpressing wild-type or mutant Trc and Rac1. Overexpression of wild-type Rac1 (RacWT) in class IV neurons resulted in overbranching of dendrites but did not produce any obvious tiling phenotype (Figures 8A, 8F, and 8G). This overbranching phenotype was partially suppressed by coexpression of wild-type Trc (Figures 8B and 8F). Importantly, whereas expressing the dominant-negative Rac1 (RacN17) alone did not cause a detectable dendritic phenotype, RacN17 significantly suppressed the overbranching phenotype but not the tiling phenotypes in neurons expressing the domi-

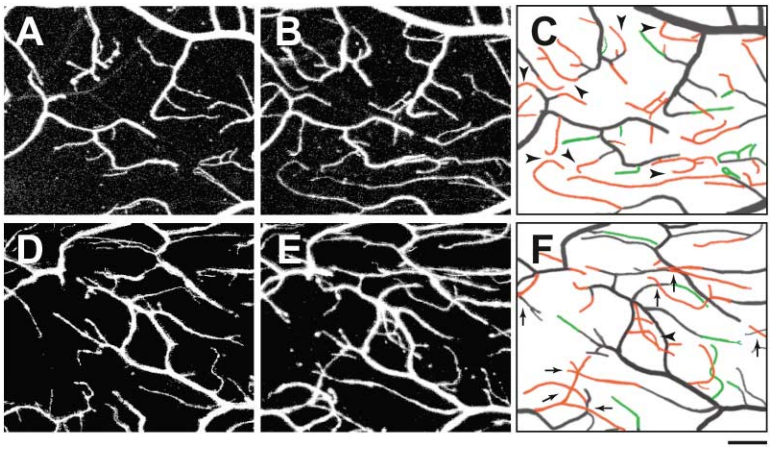

Figure 5. *fry* Mutants Are Defective in Like-Dendrite Avoidance Response

Timelapse images collected in a 16 hr interval of wild-type (A–C) and *fry*^{1} (D–F) dendrites. The images show the boundary between v'ada and vdaB dendrites. Zero-hour (A and D) and sixteen-hour (B and E) time points are shown. The dynamic branches are categorized as extension (red) and retraction (green) (C and F). Gray indicates the nondynamic portion of the arbor. Arrowheads and arrows indicate the extended branches with turning and crossing points, respectively. The scale bar represents 10 μm.

nant-negative Trc(K112A) mutant (Figures 8C, 8D, 8F, and 8G). The involvement of Rac in Trc signaling appeared specific; coexpression of the dominant-negative RhoL (RhoN25) did not result in a significant change of dendritic branching and tiling phenotypes in neurons expressing the K112A mutant (Figures 8E and 8F). These results suggest that Trc/Fry may negatively regulate Rac signaling to control dendritic branching.

To further test this possibility, we carried out coimmunoprecipitation experiments and found Trc in a complex with Rac1 but not with Cdc42 in *Drosophila* S2 cells (Figure 8H). Moreover, using a pull-down assay in which Rac-GTP (the activated form of Rac) but not Rac-GDP is isolated via the Rac-GTP binding domain of PAK conjugated to GST (Geisbrecht and Montell, 2004), we found that overexpression of wild-type Trc in stably transfected cell lines caused a significant reduction of the amount of Rac1-GTP compared to control cells, whereas expression of the dominant-negative Trc(K112A) mutant increased Rac1-GTP level (Figure 8I). Taken together, these findings suggest that the Trc/Fry signaling negatively regulates Rac activity to control dendritic branching whereas another, distinct pathway mediates the action of Trc in tiling.

Discussion

Trc and Fry in Dendritic Branching

In this study, we examined the role of Trc and Fry in patterning of the dendritic field of *Drosophila* sensory neurons. We found that the Trc/Fry signaling pathway plays an essential role in regulation of dendritic branching.

Table 1. Behavior of Dendritic Branch

	Turning	Crossing	Others	
WT	73.0%	1.1%	25.8%	(n = 178)
fry^{1}	25.6%	44.2%	30.2%	(n = 129)
fry^{6}	21.4%	46.4%	32.1%	(n = 112)

Quantification of dendritic branch behavior when their tips came close (<5 μm) to other branches. "Turning" categorizes branches that obviously turn (>90°) when their tips are extended close to other branches. "Others" categorizes the branches with no obvious turning when their tips come close to other branches and potentially includes stopping, retracting, and growing branches.

trc and *fry* mutants typically displayed excessive terminal branches, whereas the major dendrite architecture appeared normal in all four classes of da neurons. For example, the primary, secondary, and tertiary branches of class IV neurons did not show overbranching in *trc* and *fry* mutants whereas the terminal branches were increased by a factor of two. It is thus likely that Trc and Fry specifically regulate the branching of fine structures, but not overall architecture, of dendrites. Consistent with this idea, no obvious defect was observed in neurons with simple dendrites, such as bipolar neurons, external sensory neurons, and chordotonal neurons.

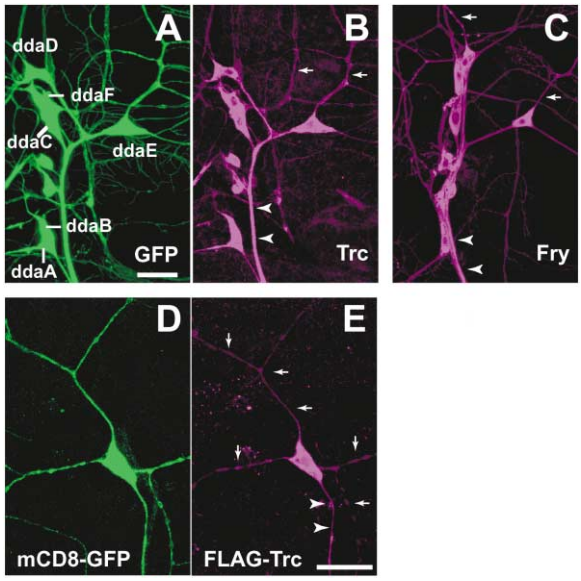

Figure 6. Expression of Trc and Fry

(A and B) Expression of endogenous Trc protein in third instar larvae. Third instar larvae expressing mCD8-GFP in all da neurons (A, green) were stained with anti-Trc antibody (B, magenta). Names of da neurons in dorsal cluster are given in white.

(C) Expression of endogenous Fry protein in wild-type third instar larvae. Arrows and arrowheads indicate dendrites and axons, respectively.

(D and E) Distribution of FLAG-tagged Trc protein overexpressed in class IV ddaC neuron. Third instar larvae carrying mCD8-GFP marker in all da neurons (E, green) were stained with anti-FLAG antibody (D, magenta). The scale bars represent 25 μm.

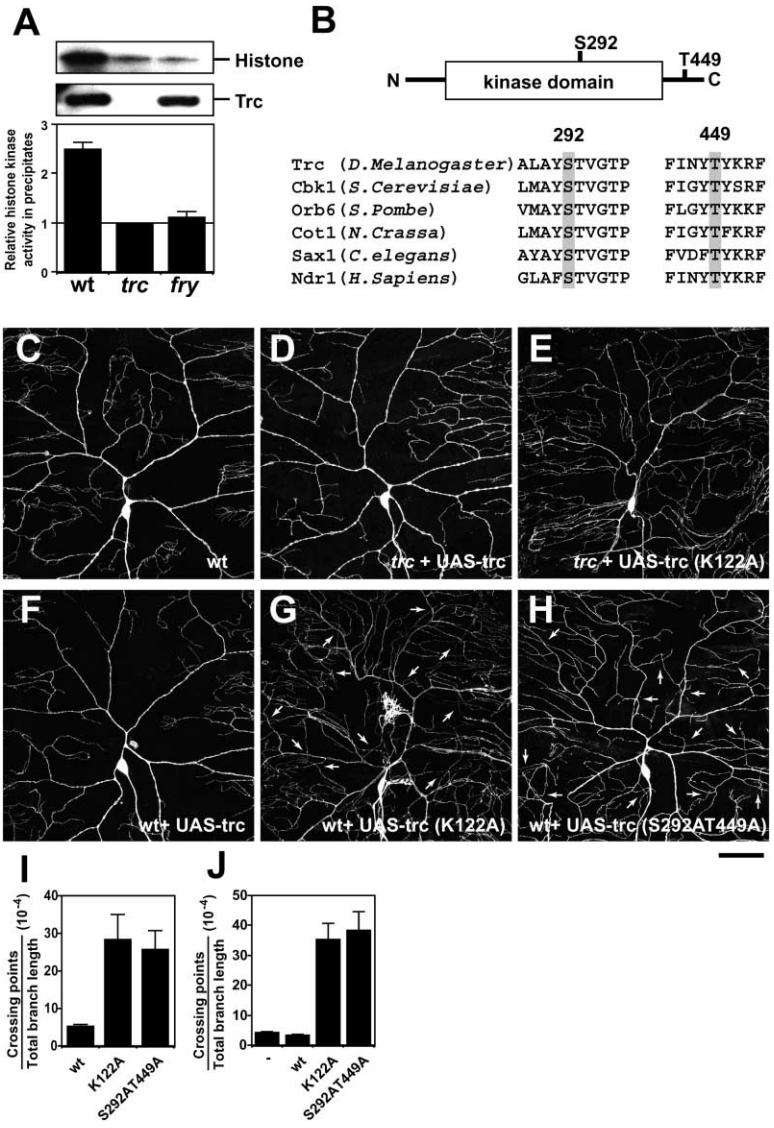

Figure 7. Trc Kinase Activity Is Essential for Dendritic Branching and Tiling Control In Vivo

(A) Trc kinase activity is dependent on Fry. Top panel shows phosphorylation of histone H1 by precipitates from wild-type (wt), *trc*^{2}, and *fry*^{1} embryos in vitro. Bead bound histone H1 kinase activity was quantified by a densitometer. The densitometer analysis of an anti-Trc blot of precipitates (middle) was used to estimate Trc level. The histone H1 kinase activities normalized to those of *trc* mutant are plotted in the graph (bottom). The means ± SD are shown (n = 3).

(B) Alignment of phosphorylation sites of Trc homologs.

(C–H) Neuronal expression of Trc mutants phenocopies the *trc/fry* mutant phenotype. (C) Wild-type ddaC neuron expressing mCD8-GFP under the control of class IV neuron-specific driver *Gal4*$^{4\text{-}77}$. (D) In *trc*^{1} mutants carrying a UAS-*trc* transgene under the control of *Gal4*$^{4\text{-}77}$ driver, ddaC dendrites was almost indistinguishable from those of wild-type. (E) In *trc*^{1} mutants carrying a UAS-*trc* (K122A) kinase-dead transgene under the control of *Gal4*$^{4\text{-}77}$ driver, no rescue was observed. (F) In wild-type larvae overexpressing Trc via *Gal4*$^{4\text{-}77}$ driver, ddaC dendrites became slightly simplified. (G and H) In wild-type larvae overexpressing Trc (K122A) (G) or (S292AT449A) (H), ddaC dendrites exhibited the increased branching and tiling defects similar to *fry/trc* mutant phenotypes. The scale bar represents 50 μm.

(I and J) Quantification of the dendritic crossing points in the rescue (I; n = 5) and the overexpression (J; n = 15) experiments.

Trc and Fry homologs have been identified in a variety of species including *S. cerevisiae* (Colman-Lerner et al., 2001; Weiss et al., 2002; Du and Novick, 2002), *S. pombe* (Verde et al., 1998; Hirata et al., 2002), *N. Crassa* (Yarden et al., 1992), *C. elegans* (Zallen et al., 2000; Gallegos and Bargmann, 2004), *Drosophila* (Geng et al., 2000; Cong et al., 2001), and mammals (Tamaskovic et al., 2003). Moreover, Fry homologs show a strong genetic interaction with Trc homologs. In *S. cerevisiae* and *S. pombe*, mutations in either of these genes cause severe cell growth defect as well as cell morphology defect. In *Drosophila*, however, other than the dendritic branching phenotype in neurons, we could not find obvious cell growth defects in any tissues in the *trc* and *fry* mutant third instar larvae (data not shown). Zallen et al. (2000) reported that mutations in the *trc* homolog *sax-1* gene cause extra neurite formation in sensory neurons of *C. elegans* while the overall structure of the neuron appears normal. Thus, the Trc/Fry signaling appears to mediate similar functions in sensory neurons of flies and worms. In addition, mutations of *trc* or *fry* result in branched bristles and multiple wing hair phenotypes in *Drosophila* (Geng et al., 2000; Cong et al., 2001), and mutation of a fungal homolog of *trc*, *cot1*, causes a drastic increase of the hyphal branching in *Neurospora* (Yarden et al., 1992). Thus, the Trc/Fry signaling is likely to be a general mechanism to regulate branching of cellular processes.

Trc and Fry Regulate Dendritic Tiling in Da Neurons

Dendritic tiling has been proposed to play a key role in patterning the dendritic fields of particular neurons, including *Drosophila* class IV sensory neurons (Jan and Jan, 2003; Grueber and Jan, 2004). Previous studies suggest that tiling in class IV neurons arises from repulsion between homologous dendrites (Grueber et al., 2003a; Sugimura et al., 2003). Consistent with this idea, our timelapse study revealed no overlap of the dendrites in late embryonic, first, second, or third instar larval stages, suggesting that tiling in class IV neurons is es-

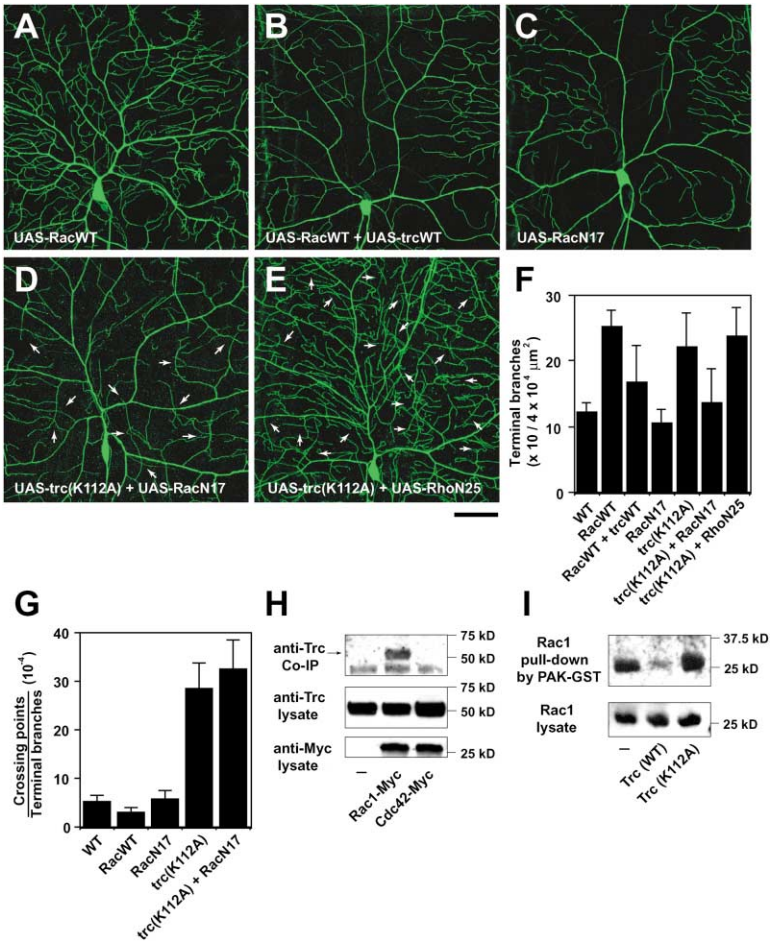

Figure 8. Trc Negatively Regulates Rac Signaling to Control Dendritic Branching

(A–E) Trc has a negative genetic interaction with Rac. Live imaging of dendrites of a class IV neuron expressing RacWT (A), RacWT and wild-type Trc (B), the dominant-negative RacN17 (C), the dominant-negative Trc (K112A) and the dominant-negative RacN17 (D), and the dominant-negative Trc (K112A) and the dominant-negative RhoN25 (E). Arrows indicate dendritic branches cross one another. The scale bar represents 50 μm. Genotypes: *yw*, *UAS-Rac1WT*; *Gal4$^{4-77}$*, *UAS-mCD8GFP/+* (A); *yw*, *UAS-Rac1WT*; *Gal4$^{4-77}$*, *UAS-mCD8GFP/+; UAS-trcWT/+* (B); *Gal4$^{4-77}$*, *UAS-mCD8GFP/+; UAS-Rac1N17/+* (C); *Gal4$^{4-77}$*, *UAS-mCD8GFP/+; UAS-trcK112A/ UAS-Rac1N17* (D); *Gal4$^{4-77}$*, *UAS-mCD8GFP/UAS-RhoLN25; UAS-trcK112A/+* (E).

(F and G) Quantification of the terminal branch number (F) and the number of dendritic crossing normalized by the terminal branch number (G) (WT, n = 15; others, n = 25).

(H) Complex formation by Trc and Rac1. *Drosophila* S2 cells were transfected by either Rac1-Myc or Cdc42-Myc or neither (—) and the lysates were immunoprecipitated by using anti-Myc antibody. Top panel shows endogenous Trc coimmunoprecipitated with Rac1-Myc but not Cdc42-Myc. The arrow indicates endogenous Trc protein. Middle panel shows endogenous Trc in cell lysates. Bottom panel shows Rac1-Myc or Cdc42-Myc in cell lysates.

(I) Trc suppresses Rac1 activity in S2 cells. S2 cells expressing wild-type Trc (WT) or the dominant-negative Trc mutant (K112A) were lysed and the extracts were incubated with GST-PAK beads, which would pull down activated Rac1 (Rac1-GTP). Top panel shows the relative amounts of the activated Rac1 (Rac1-GTP) in control S2 cells (—), S2 cells overexpressing wild-type Trc (Trc [WT]), or the dominant-negative Trc (Trc [K112A]). Bottom panel shows Rac1 in cell lyates of each cell line. The Rac-GTP (top) and total Rac1 protein (bottom) were detected by anti-Rac1 antibody.

tablished when dendrites first meet and maintained throughout the larval stage.

We have provided genetic and molecular evidence that Trc and Fry play a crucial role in establishing and maintaining the dendritic tiling of class IV neurons. In *trc* or *fry* mutants, terminal branches of class IV dendrites fail to avoid crossing each other, not only within the same neuron, but also between different neurons, leading to a significant overlap of dendritic fields. Since *trc* and *fry* null mutants display both overbranching and tiling phenotypes, one obvious possibility is that the tiling phenotype simply results from the overbranching phenotype. The following lines of evidence support the notion that the dendritic tiling defect in *trc* and *fry* mutants is not secondary to the overbranching phenotype. First, when normalized by the total branch number or the total branch length, the number of dendritic crossings in *trc* and *fry* null mutants remains significantly greater than that in wild-type controls. Second, in the absence of dendritic overbranching, a robust tiling phenotype is still observed in the *fry^{6}* hypomorphic allele, as well as larvae transheterozygous for *fry^{1}*and *fry^{6}* or for *fry^{1}* and *trc^{1}*. Third, *trc* and *fry* mutants display not only iso-neuronal tiling defects but also hetero-neuronal tiling defects (Figure 4). Such a significant overlap of the dendritic fields between neighboring class IV neurons is unlikely to result from a simple increase of terminal dendritic branches if each dendritic branch retains a like-repels-like activity. Indeed, a series of mutants, such as *flamingo* (Gao et al., 2000) and *sequoia* (Brenman et al., 2001), with dendritic overgrowth and/or overbranching have been isolated in previous studies (Gao et al., 1999); however, they appear not to have tiling defects in class IV dendrites (Grueber et al., 2002). The independence of tiling and branching phenotypes is further supported by the observation that the dominant-negative RacN17 could suppress the dendritic branching but not the tiling phenotype due to expression of the dominant-negative TrcK112A mutant.

Our timelapse observations show that in wild-type larvae, ~70% of terminal branches appeared to make a dramatic turn before they cross nearby branches, again supporting the idea that the like-repels-like mechanism plays a central role in class IV dendritic tiling. Compared to wild-type, *fry* mutant dendrites failed to turn away from nearby branches, but they showed normal net growth and retraction. Taken together, these data strongly suggest a role of Trc and Fry in the like-repels-

like behavior of the class IV dendrites. It remains possible, however, that other mechanisms function in parallel with the Trc/Fry signaling pathway to establish tiling since some dendritic branches of class IV neurons still appear to tile in *trc* and *fry* mutants.

Gallegos and Bargmann (2004) recently reported that Sax-1 and Sax-2 (the worm homologs of Trc and Fry) also have an essential role in mechanosensory neurite tiling. This finding, together with our study, strongly suggests an evolutionarily conserved role for the Trc/Fry signaling pathway in dendritic tiling. Indeed, of the two mammalian *trc* homologs *ndr1* and *ndr2*, *ndr2* is highly expressed in various tissues including the brain, while *ndr1* displays a relatively specific localization in muscles (Devroe et al., 2004). Although it has not been established whether a tiling mechanism contributes to dendritic field specification in the central nervous system outside of retina, cerebral cortical neurons are known to exhibit contact-mediated growth inhibition of neurites (Sestan et al., 1999). It will be of interest to examine potential roles of Trc and Fry homologs in regulation of dendritic tiling as well as branching in vertebrate nervous systems. Additionally, considering a close correlation between abnormal dendrite patterning and mental retardation (Purpura, 1975; Kaufmann and Moser, 2000), it might be intriguing to examine the relationship between *ndr1/2* genes and mental retardation diseases.

Trc and Fry Control Dendritic Branching and Tiling through Different Signaling Pathways

The MARCM analyses and the rescue studies, together with the expression of Trc and Fry in da neurons, indicate that Trc and Fry function cell autonomously in neurons. In addition, Trc kinase activity is indispensable for the control of dendritic branching and tiling in vivo, and Fry is required for Trc kinase activity, indicative of an important role of intracellular kinase signaling. The kinase domain of Trc is closely related to Rho-kinase (Rok), with 45% amino acid identity and 71% similarity to *Drosophila* Rok (Drok) (Winter et al., 2001), but Trc lacks a Rho binding domain and other regulatory domains (Tamaskovic et al., 2003). Indeed, *C. elegans* Sax-1 has a partial genetic interaction with Rho in neuronal cell shape regulation (Zallen et al., 2000). Whereas no obvious interaction between Trc/Fry and Rho/Drok was observed in *Drosophila* da neurons (Figure 8, data not shown), Rac signaling likely plays an important role in Trc/Fry regulation of dendritic branching of class IV neurons. Trc partially suppressed the overbranching phenotype induced by RacWT. Moreover, the dominant-negative RacN17 suppressed the overbranching but not tiling phenotypes in neurons expressing dominant-negative Trc mutant. One possible scenario is that Trc/Fry negatively regulates Rac to control dendritic branching. This notion is further supported by analyses of the active RacGTP protein level in cells expressing wild-type or mutant Trc (Figure 8).

In contrast to the involvement of Rac in dendritic branching, there is no indication that tiling depends on Rac signaling. Rather, two distinct pathways seem to be employed by Trc/Fry to control dendritic branching and tiling. This idea is consistent with our genetic data indicating that tiling defects can be separated from branching defects in *trc* and *fry* mutants. It is of interest to note that in budding yeast, Cbk1p (Trc homolog) and Tao3p (Fry homolog) play multiple roles involving different downstream pathways (Colman-Lerner et al., 2001; Weiss et al., 2002; Nelson et al., 2003).

The repulsion between dendrites likely involves either contact-mediated dendritic interactions or signaling via a short-range diffusible substance—a signal that is likely to have class-specific components (Lohmann and Wong, 2001; Jan and Jan, 2003). It is unlikely that Trc and Fry determine the class specificity since Trc and Fry are expressed in all da neurons (Figure 6). Conceivably, Trc may transmit subtype-specific repulsion signals, generated by class-specific factors to downstream components including the cytoskeleton, and induce a like-repels-like behavior of dendrites. The finding that Fry and Trc are involved in the like-repels-like response in class IV neurons has provided an entry point for studying the molecular mechanisms that control dendritic tiling. As shown in this study, phosphorylation of the conserved Ser/Thr of Trc appears critical for the Trc/Fry signaling in vivo, yet little is known about the upstream kinase(s) and the downstream substrate(s) of Trc in any species. A molecular dissection of the Trc kinase signaling pathway in neurons will help us to elucidate how the Trc/Fry signaling pathway governs dendritic branching and tiling.

Experimental Procedures

Fly Stocks

For visualizing class IV dendrites, we used *pickpocket (ppk)-GFP* (Grueber et al., 2003a), *ppk-GFP; fry^{1}/TM6B Tb*, and *ppk-GFP*; *trc^{1}/TM6B Tb*. *trc* mutants were generated by PCR-based site-directed mutagenesis. *trc* and mutants were subcloned into pUAST to generate UAS-*flag-trc* and mutants. *yw; Gal4$^{4\text{-}77}$*, UAS-*mCD8-GFP* flies were used for ectopic expression of Trc and mutants in class IV neurons. *fry^{1}* and *trc^{1}* are null alleles produced by a chemical mutagenesis (Geng et al., 2000; Cong et al., 2001). *fry^{6}* is a hypomorphic allele with a significant decrease in *fry* mRNA level, which was generated by a P element insertion. *trc^{7}* is a null allele generated by a P element insertion (Geng et al., 2000). The *trc fry* double mutant was generated by recombination of *trc^{7}* with *fry^{1}* (Cong et al., 2001). Rac mutants and transgenic lines are a gift from Liqun Luo. The UAS-RhoN25 transgenic line is from Bloomington Stock Center.

MARCM Analysis

MARCM analyses were performed as described previously with some modifications (Grueber et al., 2002). In brief, to generate mosaic mutant clones, *fry^{1}, FRT^{80B}/TM6C*, *trc^{1}, FRT^{80B}/TM6C,* or *trc^{7} fry^{1}, FRT^{80B}/TM6C* flies were mated with *w*; *elav-Gal4*, *hsFLP*; *FRT^{80B}*, *tub-Gal80/TM6B*. For the wild-type clones, *w*; p[*FRT^{80B}*] flies were mated to *w*; *elav-Gal4*, *hsFLP*; *FRT^{80B}*, *tub-Gal80/TM6B*. Embryos were collected for 2 hr and allowed to develop for 3–5 hr at 25°C before a heat shock. The heat shock was performed at 38°C for 45 min, followed by room temperature recovery for 30 min, and an additional exposure to 38°C for 45 min. The eggs were kept in 25°C and third instar larvae were examined for mutant clones and then dissected, fixed, and stained with rat anti-mCD8 antibody (1:200 dilution; Caltag, Burlingame, California). The stained larvae were mounted in DPX. Fluorescence images were obtained by confocal microscopy (Leica TCS SP2).

Immunocytochemistry

Anti-Trc antibody was generated by immunization of guinea pigs with a GST-Trc fusion protein containing the N-terminal 200 amino acids of Trc. Anti-Fry antibody was generated in rats immunized with a peptide corresponding to the N-terminal 20 amino acids of Fry. Third instar larvae of *yw*; *Gal4$^{109(2)80}$*, UAS-*mCD8-GFP* flies, which

express mCD8-GFP in all md neurons (Gao et al., 1999), were dissected, fixed, and stained with purified anti-Trc antibody (1:50,000 dilution) or purified anti-Fry antibody (1:100), and subsequently with rhodamine-conjugated goat anti-guinea pig or -rat IgG antibody (1:200).

Kinase Assay

Embryos (stage 16/17) homogyzous for *fry*^{1} or *trc*^{2} (null allele; no detectable *trc* mRNA caused by a point mutation in the first intron of *trc* gene) were selected by their lack of a GFP-expressing balancer chromosome. Approximately 200 embryos were homogenized in 100 μl of Lysis buffer A (150 mM NaCl, 50 mM Tris-HCl, pH7.4, 2 mM EDTA, 1% Triton X-100, 10% glycerol, 2 mM dithiothreitol, 1 mM benzamide, 1 mM PMSF, 10 mM NaF, 20 mM β-glycerophosphate, 2 mM Na_3VO_4, and Complete protease inhibitor cocktail [Roche]). Lysates were centrifuged at 10,000 × g for 15 min and the supernatants were precleared by protein A-Sepharose for 1 hr. The supernatants were incubated with anti-Trc antibody for 2 hr and then with protein A-Sepharose for 1 hr. The beads were then washed with lysis buffer six times and with kinase buffer (20 mM Tris-HCl, pH 7.4, 10 mM $MgCl_2$, 1 mM dithiothreitol, 100 μM ATP) three times. Thereafter, beads were incubated in kinase buffer containing 10 μCi of [γ-^{32}P]ATP and 2 μg of histone H1.

Immunoprecipitation

Transfection was performed by using Fugen 6 reagent (Roche). Two days after transfection, cells were lysed in Lysis buffer A and spun at 5,000 × g for 15 min. Extracts were precleaned by Protein G-Agarose beads (Roche) and then incubated with primary antibodies for 2 hr, followed by Protein G beads for 1 hr. Beads were washed five times in lysis buffer for analyses of associated proteins by SDS-PAGE and Western blot.

Rac Activation Assay

Full-length cDNA coding for *trc* was amplified by PCR and subcloned into the pMt-V5/His vector (Invitrogen). The *trc* mutants were generated by PCR-based site-direct mutagenesis. S2 cells were cotranfected with pMt-*trc* or pMT-*trc* mutants and pCoHyg (a hygromycin-resistant vector; Invitrogen), and the stable cell lines were selected by culturing in the hygromycin-containg growth media for one month. For activated Rac pull-down assay, cells were incubated with 500 μM $CuSO_4$ for 24 hr and then lysed in Mg^{2+} lysis buffer (50 mM Hepes, pH 7.4, 100 mM NaCl, 1% Triton X-100, 10 mM $MgCl_2$, 1 mM EDTA, 5% glycerol, 20 mM β-glycerophosphate, 1 mM dithiothreitol, and Complete cocktail) and spun at 5,000 × g for 15 min. The extracts were incubated with GST-PAK (aa 59–272) beads (Geisbrecht and Montell, 2004) for 2 hr and washed five times with Mg^{2+} buffer before Western blot. The blot was performed by using anti-Rac1 antibody (Luo et al., 1994; Geisbrecht and Montell, 2004).

Acknowledgments

We thank L. Luo, D. Montell, A. Chiba, K. Kaibuchi, and Bloomington Stock Center for fly stocks and reagents; H.-J. Chung for helpful suggestion on in vitro kinase assay; J. Parrish for critical comments on the manuscript; S. Younger for advice on fly genetics; and members of the Jan Lab for stimulating discussion. We also thank M. Gallegos and C. Bargmann for communicating their results before publication. This work is supported by NIH grant R01NS40929 (Y.-N.J.) and R0153498 (P.N.A.). K.E. is a research associate and Y.-N.J. and L.Y.J. are investigators of Howard Hughes Medical Institute.

Received: April 24, 2004
Revised: August 10, 2004
Accepted: August 30, 2004
Published: October 14, 2004

References

Adler, P.N. (2002). Planar signaling and morphogenesis in *Drosophila*. Dev. Cell *2*, 525–535.

Bodmer, R., and Jan, Y.N. (1987). Morphological differentiation of the embryonic peripheral neurons in *Drosophila*. Rouxs Arch. Dev. Biol. *196*, 69–77.

Brenman, J.E., Gao, F.B., Jan, L.Y., and Jan, Y.N. (2001). Sequoia, a tramtrack-related zinc finger protein, functions as a pan-neural regulator for dendrite and axon morphogenesis in *Drosophila*. Dev. Cell *1*, 667–677.

Cline, H.T. (2001). Dendritic arbor development and synaptogenesis. Curr. Opin. Neurobiol. *11*, 118–126.

Colman-Lerner, A., Chin, T.E., and Brent, R. (2001). Yeast Cbk1 and Mob2 activate daughter-specific genetic programs to induce asymmetric cell fates. Cell *107*, 739–750.

Cong, J., Geng, W., He, B., Liu, J., Charlton, J., and Adler, P.N. (2001). The *furry* gene of *Drosophila* is important for maintaining the integrity of cellular extensions during morphogenesis. Development *128*, 2793–2802.

DeVries, S.H., and Baylor, D.A. (1997). Mosaic arrangement of ganglion cell receptive fields in rabbit retina. J. Neurophysiol. *78*, 2048–2060.

Devroe, E., Erdjument-Bromage, H., Tempst, P., and Silver, P.M. (2004). Human Mob proteins regulate the Ndr1 and Ndr2 serine-threonine kinases. J. Biol. Chem. *279*, 24444–24451.

Du, L.L., and Novick, P. (2002). Pag1p, a novel protein associated with protein kinase Cbk1p, is required for cell morphogenesis and proliferation in *Saccharomyces cerevisiae*. Mol. Biol. Cell *13*, 503–514.

Gallegos, M.E., and Bargmann, C.I. (2004). Mechanosensory neurite termination and tiling depend on SAX-2 and the SAX-1 kinase. Neuron *44*, 239–249.

Gao, F.B., Brenman, J.E., Jan, L.Y., and Jan, Y.N. (1999). Genes regulating dendritic outgrowth, branching, and routing in *Drosophila*. Genes Dev. *13*, 2549–2561.

Gao, F.B., Kohwi, M., Brenman, J.E., Jan, L.Y., and Jan, Y.N. (2000). Control of dendritic field formation in *Drosophila*: the role of Flamingo and competition between homologous neurons. Neuron *28*, 91–101.

Geisbrecht, E.R., and Montell, D.J. (2004). A role for *Drosophila* IAP-1 mediated caspase inhibition in Rac-dependent cell migration. Cell *118*, 111–125.

Geng, W., He, B., Wang, M., and Adler, P.N. (2000). The *tricornered* gene, which is required for the integrity of epidermal cell extensions, encodes the *Drosophila* nuclear DBF2-related kinase. Genetics *156*, 1817–1828.

Grueber, W.B., and Jan, Y.N. (2004). Dendritic development: lessons from *Drosophila* and related branches. Curr. Opin. Neurobiol. *14*, 74–82.

Grueber, W.B., Graubard, K., and Truman, J.W. (2001). Tiling of the body wall by multidendritic sensory neurons in *Manduca sexta*. J. Comp. Neurol. *440*, 271–283.

Grueber, W.B., Jan, L.Y., and Jan, Y.N. (2002). Tiling of the *Drosophila* epidermis by multidendritic sensory neurons. Development *129*, 2867–2878.

Grueber, W.B., Ye, B., Moore, A., Jan, L.Y., and Jan, Y.N. (2003a). Dendrites of distinct classes of *Drosophila* sensory neurons show different capacities for homotypic repulsion. Curr. Biol. *13*, 618–626.

Grueber, W.B., Jan, L.Y., and Jan, Y.N. (2003b). Different levels of the homeodomain protein Cut regulate distinct dendrite branching patterns of multidendritic neurons. Cell *112*, 805–818.

Hirata, D., Kishimoto, N., Suda, M., Sogabe, Y., Nakagawa, S., Yoshida, Y., Sakai, K., Mizunuma, M., Miyakawa, T., Ishiguro, J., and Toda, T. (2002). Fission yeast Mor2/Cps12, a protein similar to *Drosophila* Furry, is essential for cell morphogenesis and its mutation induces Wee1-dependent G2 delay. EMBO J. *21*, 4863–4874.

Jan, Y.N., and Jan, L.Y. (2003). The control of dendrite development. Neuron *40*, 229–242.

Kaufmann, W.E., and Moser, H.W. (2000). Dendritic anomalies in disorders associated with mental retardation. Cereb. Cortex *10*, 981–991.

Lee, A., Li, W., Xu, K., Bogert, B.A., Su, K., and Gao, F.B. (2003). Control of dendritic development by the *Drosophila* fragile X-related

gene involves the small GTPase Rac1. Development *130*, 5543–5552.

Lee, T., and Luo, L. (1999). Mosaic analysis with a repressible cell marker for studies of gene function in neuronal morphogenesis. Neuron *22*, 451–461.

Lee, T., Winter, C., Marticke, S.S., Lee, A., and Luo, L. (2000). Essential roles of *Drosophila* RhoA in the regulation of neuroblast proliferation and dendritic but not axonal morphogenesis. Neuron *25*, 307–316.

Li, Z., Van Aelst, L., and Cline, H.T. (2000). RhoGTPases regulate different aspects of dendritic arbor growth in Xenopus central neurons in vivo. Nat. Neurosci. *3*, 217–225.

Lohmann, C., and Wong, R.O. (2001). Cell-type specific dendritic contacts between retinal ganglion cells during development. J. Neurobiol. *48*, 150–162.

MacNeil, M.A., and Masland, R.H. (1998). Extreme diversity among amacrine cells: implications for function. Neuron *20*, 971–982.

Luo, L. (2002). Actin cytoskeleton regulation in neuronal morphogenesis and structural plasticity. Annu. Rev. Cell Dev. Biol. *18*, 601–635.

Luo, L., Liao, Y.J., Jan, L.Y., and Jan, Y.N. (1994). Distinct morphogenesis functions of similar small GTPases: *Drosophila* Drac1 is involved in axonal outgrouwth and myoblast fusion. Genes Dev. *8*, 1787–1802.

Millward, T.A., Hess, D., and Hemmings, B.A. (1999). Ndr protein kinase is regulated by phosphorylation on two conserved sequence motifs. J. Biol. Chem. *274*, 33847–33850.

Nakayama, A.Y., Harms, M.B., and Luo, L. (2000). Small GTPases Rac and Rho in the maintenance of dendritic spines and branches in hippocampal pyramidal neurons. J. Neurosci. *20*, 5329–5338.

Nelson, B., Kurischko, C., Horecka, J., Mody, M., Nair, P., Pratt, L., Zougman, A., McBroom, L.D.B., Hughes, T.R., Boone, C., and Luca, F.C. (2003). RAM: A conserved signaling network that regulates Ace2p transcriptional activity and polarized morphogenesis. Mol. Biol. Cell *14*, 3782–3803.

Perry, V.H., and Linden, R. (1982). Evidence for dendritic competition in the developing retina. Nature *297*, 683–685.

Purpura, D.P. (1975). Dendritic differentiation in human cerebral cortex: normal and aberrant developmental patterns. Adv. Neurol. *12*, 91–116.

Redmond, L., and Ghosh, A. (2001). The role of Notch and RhoGTPase signaling in the control of dendritic development. Curr. Opin. Neurobiol. *11*, 111–117.

Scott, E.K., and Luo, L. (2001). How do dendrites take their shape? Nat. Neurosci. *4*, 359–365.

Sestan, N., Artavanis-Tsakonas, S., and Rakic, P. (1999). Contact-dependent inhibition of cortical neurite growth mediated by Notch signaling. Science *286*, 741–746.

Sugimura, K., Yamamoto, M., Niwa, R., Satoh, D., Goto, S., Taniguchi, M., Hayashi, S., and Uemura, T. (2003). Distinct developmental modes and lesion-induced reactions of dendrites of two classes of *Drosophila* sensory neurons. J. Neurosci. *23*, 3752–3760.

Tamaskovic, R., Bichsel, S.J., and Hemmings, B.A. (2003). NDR family of AGC kinases-essential regulators of the cell cycle and morphogenesis. FEBS Lett. *546*, 73–80.

Threadgill, R., Bobb, K., and Ghosh, A. (1997). Regulation of dendritic growth and remodeling by Rho, Rac, and Cdc42. Neuron *19*, 625–634.

Van Aelst, L., and Cline, H.T. (2004). RhoGTPases and activity-dependent dendrite development. Curr. Opin. Neurobiol. *14*, 297–304.

Verde, F., Wiley, D.J., and Nurse, P. (1998). Fission yeast orb6, a ser/thr protein kinase related to mammalian rho kinase and myotonic dystrophy kinase, is required for maintenance of cell polarity and coordinates cell morphogenesis with the cell cycle. Proc. Natl. Acad. Sci. USA *95*, 7526–7531.

Wässle, H., and Boycott, B.B. (1991). Functional architecture of mammalian retina. Physiol. Rev. *71*, 447–478.

Wässle, H., Peichel, I., and Boycott, B.B. (1981). Dendritic territories of cat retinal ganglion cells. Nature *292*, 344–345.

Weiss, E.L., Kurischko, C., Zhang, C., Shokat, K., Drubin, D.G., and Luca, F.C. (2002). The Saccharomyces cerevisiae Mob2p-Cbk1p kinase complex promotes polarized growth and act with the mitotic exit network to facilitate daughter cell-specific localization of Ace2p transcription factor. J. Cell Biol. *158*, 885–900.

Whitford, K.L., Dijkhuizen, P., Polleux, F., and Ghosh, A. (2002). Molecular control of cortical dendrite development. Annu. Rev. Neurosci. *25*, 127–149.

Winter, C.G., Wang, B., Ballew, A., Royou, A., Karess, R., Axelrod, J.D., and Luo, L. (2001). *Drosophila* Rho-associated kinase (Drok) links Frizzled-mediated planar cell polarity signaling to the actin cytoskeleton. Cell *105*, 81–91.

Yarden, O., Plamann, M., Ebbole, D.J., and Yanofsky, C. (1992). *cot-1*, a gene required for hyphal elongation in *Neurospora crassa*, encodes a protein kinase. EMBO J. *11*, 2159–2166.

Ye, B., Petritsch, C., Clark, I.E., Gavis, E.R., Jan, L.Y., and Jan, Y.N. (2004). *nanos* and *pumilio* are essential for dendrite morphogenesis in *Drosophila* peripheral neurons. Curr. Biol. *14*, 314–321.

Zallen, J.A., Peckol, E.L., Tobin, D.M., and Bargmann, C.I. (2000). Neuronal cell shape and neurite initiation are regulated by the Ndr kinase SAX-1, a member of the Orb6/COT-1/warts serine/threonine kinase family. Mol. Biol. Cell *11*, 3177–3190.